TITLE PAGE

Non-destructive egg breed separation using advanced VOC analytical techniques HSSE-GC-MS, PTR-TOF-MS, and SIFT-MS: assessment of performance and systems' complementarity

Matthias Corion[a], Miguel Portillo-Estrada[b], Simão Santos[a], Jeroen Lammertyn[a], Bart De Ketelaere[c], Maarten Hertog[d,1]

[a] KU Leuven, BIOSYST-MeBioS Biosensors group, Department of Biosystems, Leuven, Belgium

[b] University of Antwerp, Research Group Pleco, Department of Biology, Wilrijk, Belgium

[c] KU Leuven, BIOSYST-MeBioS Biostatistics group, Department of Biosystems, Leuven, Belgium

[d] KU Leuven, BIOSYST-MeBioS Postharvest group, Department of Biosystems, Leuven, Belgium

[1] Corresponding author: E-mail: maarten.hertog@kuleuven.be Telephone: +32 16 32 16 14

ABSTRACT

Over the past decade, advanced analytical techniques have been utilized to examine volatile organic compounds (VOCs) in eggs. These VOCs offer valuable insights into factors such as freshness, fertility, the presence of cracks, embryo sex, and breed. In our study, we assessed three mass spectrometry-based systems (headspace sorptive extraction gas chromatography-mass spectrometry; HSSE-GC-MS, proton transfer reaction time-of-flight-mass spectrometry; PTR-TOF-MS; and selected ion flow tube mass spectrometry; SIFT-MS) to analyze and identify VOCs present in intact hatching eggs from three distinct breeds (Dekalb white layer, Shaver brown layer, and Ross 308 broiler). The eggs were sampled on incubation days 2 and 8, to identify VOCs that distinguish breeds irrespective of incubation day. VOC measurements were conducted on 15 eggs per breed by placing them together with PDMS-coated stir bars inside inert Teflon® air sampling bags. After an accumulation period of 2 hours, the headspace was analyzed using PTR-TOF-MS and SIFT-MS, while the VOCs adsorbed onto the stir bars were analyzed using GC-MS for additional compound identification. Partial least squares discriminant analysis (PLS-DA) models were constructed for breed differentiation, and variable selection was performed. As a result, 111 VOCs were identified using HSSE-GC-MS, with alcohols and esters being the most abundant. The PLS-DA models demonstrated the efficacy of breed discrimination, with the HSSE-GC-MS and the PTR-TOF-MS exhibiting the highest balanced accuracy of 95.5% using a reduced set of 11 VOCs and 5 product ion masses, respectively. The SIFT-MS model had a balanced accuracy of 92.8% with a reduced set of 11 product ion masses. Furthermore, complementarity was observed between HSSE-GC-MS, which primarily selected higher molecular weight VOCs, and PTR-TOF-MS and SIFT-MS. A higher correlation was found for compound abundances between the HSSE-GC-MS and the PTR-TOF-MS relative to the SIFT-MS, indicating that the PTR-TOF-MS was better suited to quantify specific compounds identified by the HSSE-GC-MS. Finally, the findings support the presence of VOCs originating from both synthetic and natural sources, highlighting the ability of the VOC analysis systems to non-destructively perform quality control and reveal differences in management practices or biological information encoded in eggs.

41 # KEYWORDS

42 HSSE-GC-MS, SIFT-MS, PTR-TOF-MS, Hatching eggs, Mass spectrometry, Egg breed discrimination,
43 VOC analysis

44

ABBREVIATIONS

CIS	Cooled injection system
FiPLS	Forward interval partial least squares
GC-MS	Gas chromatography-mass spectrometry
HSSE	Dynamic headspace sorptive extraction
HSSE-GC-MS	Headspace sportive extraction-gas chromatography-mass spectrometry
NIPALS	Non-linear iterative partial least squares
PLS-DA	Partial least squares-discriminant analysis
PTR-MS	Proton transfer reaction-mass spectrometry
PTR-TOF-MS	Proton transfer reaction-time-of-flight-mass spectrometry
RMSECV	Root mean square error of the cross-validation set
SIFT-MS	Selected ion flow tube-mass spectrometry
SPME	Solid phase microextraction
TDU	Thermal desorption unit
TOF-MS	Time-of-flight-mass spectrometry
VIP	Variable importance in projection
VOC	Volatile organic compound

1. Introduction

In the last decade, research has been performed on studying egg volatile organic compounds (VOCs) using advanced analytical techniques. More specifically, it has been observed that these VOCs from intact eggs can provide information related to fertility (Webster et al., 2015; Xiang et al., 2018), freshness (Liu & Tu, 2012; Yongwei et al., 2009), nutritional value (Hua et al., 2021; Zhang et al., 2022), the presence of cracks (Cheng et al., 2010), sex (Borras et al., 2023; Costanzo et al., 2016; Webster et al., 2015; Xiang et al., 2022), and breed origin (Xiang, Jin, et al., 2019). The origin of egg VOCs can be subdivided into three distinct groups. (1) Environmental VOCs can be absorbed by the egg post-laying through the cuticle, the shell, and the membranes. Subsequently, these exogenous VOCs may be re-emitted, particularly at higher temperatures (Webster et al., 2015). (2) VOCs can have a biochemical origin through the degradation of egg compounds (i.e., shell, cuticle, albumen, and yolk). More specifically, amino acids from proteins can be degraded through Strecker degradation (Belitz et al., 2009; Rizzi, 2008). Furthermore, lipid autoxidation of especially unsaturated fatty acids and oxidative degradation of carotenoids are known to give rise to VOCs as well (Belitz et al., 2009). (3) Egg VOCs may originate from biological processes if the egg is fertilized, as the metabolic activities of the growing embryo can lead to VOC production. Studies have shown that VOC profiles of fertilized eggs differ from those of unfertilized ones (Webster et al., 2015; Xiang et al., 2018). Moreover, research has shown that microbiota can be found in eggs and chicken embryos (Lee et al., 2019), which suggests that these microorganisms could also contribute to the production of VOCs.

Typically, gas chromatography-mass spectrometry (GC-MS) is regarded as the gold standard analytical system that is used for identifying sampled VOCs. Hereby, eggs are incubated in a container, and headspace extraction is performed utilizing a solid phase microextraction (SPME) fiber. After extraction, the fiber is desorbed into the inlet of the GC-MS for analysis (Costanzo et al., 2016; Webster et al., 2015; Xiang et al., 2018, 2022; Xiang, Wang, et al., 2019). Next, compound identification can be achieved through separation and mass detection. One disadvantage is that the extraction time and the subsequent analysis can be a time-

consuming procedure, which may require tens of minutes to hours for each sample (Turner, 2016). Next to the SPME fiber, other promising extraction techniques for intact egg VOC measurements exist such as dynamic headspace sorption using sorbent tubes or headspace sorptive extraction (HSSE) using sorbent stir bars. Both techniques offer better sensitivity than SPME fibers and allow for airtight capping of the sorbent material and sample storage for weeks. This facilitates the collection of a high volume of samples to be analyzed on a GC-MS at a later point in time (Turner, 2016). When exposed to high relative humidity, sorbent tubes may experience reduced VOC adsorption efficiency and decreased sensitivity (Helmig & Vierling, 1995). In contrast, sorbent stir bars have been demonstrated to exceed the sensitivity of SPME fiber measurements from the headspace of aqueous samples (Tienpont et al., 2000). As a result, it is thought to be less affected by sample moisture than the sorbent tubes and therefore ideal for measuring VOCs from intact eggs. One recent study already employed sorbent stir bars in active headspace sampling to determine the sex of the chick embryo (Borras et al., 2023).

One way of increasing the throughput of the classical GC-MS approach is by making use of direct trace gas mass spectrometers. Besides their higher cost, measurements can be performed rapidly and directly on the headspace with no need for extraction and pre-concentration with sorbent materials (Turner, 2016). Selected ion flow tube mass spectrometry (SIFT-MS) provides the option of selecting H_3O^+, NO^+, or O_2^+ reagent ions, whereas proton transfer reaction mass spectrometry (PTR-MS) typically utilizes H_3O^+ ions as precursor ions, although modern instruments may allow the use of alternative ions (Turner, 2016). These reagent ions are subsequently used to ionize sample analytes, resulting in product ions that may be separated by a mass spectrometer. Apart from generating a multivariate signal through full mass spectra for fingerprinting, individual masses can also be used for VOC identification (Smith et al., 2014). Unlike GC-MS, the identification process is not conclusive as soft chemical ionization techniques used by both instruments may generate ions that could originate from multiple compounds (Turner, 2016). Nevertheless, their benefit lies in their swift analysis speed of seconds to minutes, which enables quick screening. Relevant to our study is that the primary distinction between SIFT-MS and PTR-MS lies in the provision

of three reagent ions in SIFT-MS, thereby enhancing specificity. In the case of PTR-MS, the use of H_3O^+ as the sole reagent ion might be overcome by employing time-of-flight mass spectrometry (TOF-MS), which enables the generation of precise ion masses and, consequently, aids compound identification while also increasing specificity (Smith et al., 2014).

Our study seeks to evaluate the efficacy of three promising and distinct analysis systems in identifying the VOCs of intact eggs (i.e., HSSE-GC-MS, PTR-TOF-MS, and SIFT-MS), focussing on hatching eggs from three different chicken breeds (i.e., Dekalb white layers, Shaver brown layers, and Ross 308 broilers). Studying egg breed differentiation holds scientific importance as it implicitly enables the assessment of the quality or the egg's provenance (Xiang, Jin, et al., 2019). Xiang *et al.* (2019) differentiated three breeds of hatching eggs using SPME-GC-MS at the onset of incubation. Our study advances on this earlier research in two ways. Firstly, measurements are performed on two different days of incubation (i.e., days 2 and 8) reducing the likelihood of accidentally selecting environmental or time-specific VOCs making the approach potentially more robust. Secondly, more versatile sorbent stir bars are used for headspace extraction, followed by GC-MS analysis, with simultaneous measurements of egg VOCs on PTR-TOF-MS and SIFT-MS. To our knowledge, this is the first study that reports the use of these three highly performant VOC analysis systems on intact eggs. It is expected that the results will provide valuable insights into the performance of these instruments for non-destructively analyzing egg VOCs.

2. Materials & methods

2.1.Egg samples

All hatching eggs were purchased from Hatchery Verhaeghe – Het Anker (Wervik, Belgium). The eggs originated from around 1-year-old animals of three different breeds: Dekalb white layers (55 weeks old), Shaver brown layers (48 weeks old), and Ross 308 broilers (45 weeks old). The eggshells were inspected for damage or dirt and were cleaned with water and paper wetted with ethanol (99.8%, Thermo Fisher Scientific, Waltham, MA). Next, the eggs were left to air-dry and numbered using a pencil. A total of 15 eggs per breed was selected with a similar egg weight distribution among the breeds. Upon incubation, the eggs were stored for a maximum of 7 days after laying at 18 °C and minimally 60% relative humidity.

The eggs were incubated under standard conditions (37.7 °C and 55% relative humidity) in an RCOM max 50 DO (Autoelex Co. Ltd., Deokam-ri, Republic of Korea). During the process, they were tilted every hour, and VOC measurements were performed on incubation days 2 and 8. On these measurement days, the eggs remained in the incubator and were transported back and forth between two locations in Belgium (Wilrijk and Leuven) to perform measurements respectively on the PTR-TOF-MS device in Wilrijk in the morning and the SIFT-MS measurements in Leuven in the afternoon. On day 14, the eggs were removed from the incubator to assess fertility and embryo development. After the breakout, living embryos were decapitated with sharp scissors. The performed experiment was approved by the Animal Ethics Committee of the KU Leuven under project number ECD P025/2019.

2.2.Headspace incubation and extraction

Inert materials such as Teflon® and stainless steel were used to minimize the background signal for the VOC measurements. For the headspace accumulation, it was decided to individually enclose eggs in fluorinated ethylene propylene bags with slide-on airtight bag sealers and polypropylene valves for air sampling (Sense Trading, Groningen, Netherlands). Unlike inflexible headspace containers that require an additional air inlet to prevent vacuum pulling, the use of bags allowed sampling without the undesirable

effect of diluting the headspace. These bags were cut and resealed to a size of 125 mm by 170 mm. After each measurement, bags were emptied and resealed following a thermal cleaning procedure by which the bags were three times automatically filled with hot air at 100 °C and emptied using a thermal heat purger (Model SP20, Scentroid, Whitchurch–Stouffville, Canada). A 100 mL SGE analytical gas-tight syringe (Trajan Scientific and Medical, Ringwood, Australia), mounted with stainless steel Luer-lock valves and Polytetrafluoroethylene tubing and connectors, was used to draw air in and out of the bag. The inlet air was filtered by a Supelcarb HC hydrocarbon trap (Supelco, Bellefonte, PA), whereas the outlet air was exhausted into the room (Fig. 1A).

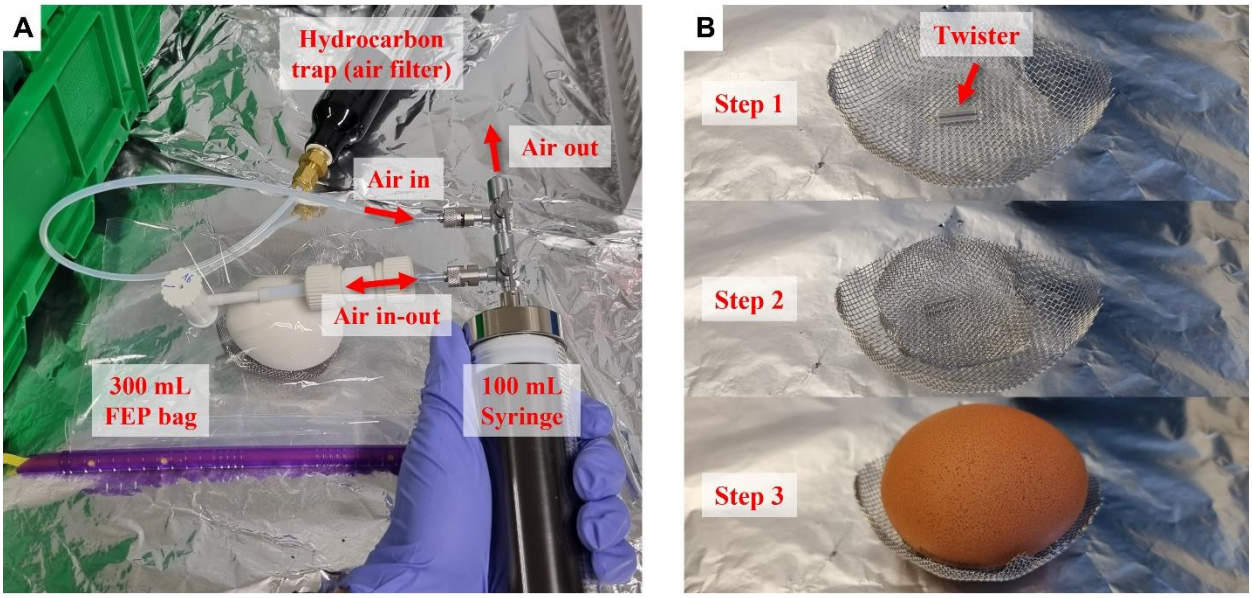

Fig. 1. Preparation of the eggs for intact headspace measurements. (A) Syringe configuration in which the airflow is indicated with arrows. The bag was flushed once before it was filled with 300 mL of filtered air. (B) Grid configuration explained in steps with the Twister® at the bottom for headspace extraction in the bag and the egg on top of it

Before enclosing the egg inside the bag, it was placed on a stainless steel grid holder under which a second holder was placed with a Gerstel polydimethylsiloxane (PDMS) Twister® (Gerstel, Mülheim an der Ruhr, Germany). These sorbent stir bars had a 1 mm thick PDMS coating and were 10 mm in length. The Twisters® were conditioned before use following manufacturer guidelines. This grid holder configuration ensured that every Twister® was securely positioned at a fixed grid-thick distance from the eggshell (Fig. 1B). After placing an egg with a Twister® inside and sealing the bag, the air was pulled out using the syringe.

Next, the bag was filled with 300 mL of filtered air and subsequently vacuum-pulled again. Finally, the bag was filled a second time with 300 mL of filtered air and it was placed in an incubator at 37.7 °C during 2 h of headspace accumulation upon analysis on the PTR-TOF-MS or SIFT-MS. During these 2 h, the Twister® extracted the egg VOCs which would be subject to further analysis on the GC-MS. During the measurement session, three blank measurements were conducted as a reference for background compounds. The blank measurements followed the same protocol but without the presence of an egg.

Following the headspace sampling for analysis, the egg was removed from the bag and returned to the egg incubator. The bag underwent the cleaning protocol for reuse and the Twister® was stored in a 60 mm length desorption tube, which was secured with a transport adapter and stored in a transport block for GC-MS analysis. The desorption tube, transport adapter, and transport block were all from Gerstel.

2.3.Device conditions and data preprocessing

2.3.1. GC-MS

The Twisters® were stored in the transport block at 21 °C for a maximum of 5 days before undergoing analysis using GC-MS. For the analysis, Twisters® were desorbed in a thermal desorption unit (TDU) connected to a cooled injection system (CIS, Gerstel). Twister® desorption occurred in the TDU under a 50 mL/min helium flow. The TDU was initially set at 25 °C and its temperature was increased at a rate of 60 °C/min up to 250 °C which was held for 5 min. The desorbed VOCs were carried via helium flow into the CIS that was maintained at -50 °C. After complete desorption, the CIS was heated at a ramp of 12 °C/s up to 300 °C and held for 5 min.

Chromatography was performed using an Agilent 7890A gas chromatograph coupled to an Agilent 5975C mass selective detector (Agilent Technologies, Santa Clara, CA). The GC-MS was equipped with a 30 m x 250 µm x 0.25 µm HP-5MS column (Agilent Technologies) operating at a helium flow rate of 1.07 mL/min. The oven program was as follows: initial setpoint at 35 °C directly followed by a first ramping at 4 °C/min up to 120 °C without hold time. A second ramping was set at 6 °C/min up to 200 min

immediately followed by a third ramp at 10 °C/min up to 250 °C with a hold time of 5 min. The mass spectrometer scanned the range from 30 to 350 m/z and the mass spectrometer source and mass spectrometer Quad were respectively set at 230 °C and 150 °C.

The chromatograms and spectra were analyzed using MassHunter Workstation (Unknowns and Quantitative Analysis v10.1, Agilent Technologies). Initially, the chromatograms were deconvoluted in the Unknowns Analysis and compounds were tentatively identified based on the NIST 2020 database by setting a minimum match factor of 85. The match factor assesses the degree of similarity between an obtained fragmentation spectrum and the theoretical fragmentation spectra of a compound in the database. The following rules were applied to retain compounds for a custom-made library: (1) a minimum match factor of 85, (2) a higher abundance in the egg measurements compared to the blank measurements, (3) a minimum occurrence of 10% across all observations or significant differences in one of the breeds based on a pairwise t-test, and (4) their presence in previous in-house experiments on egg VOCs. In the second step, these compounds were double-checked for having a realistic retention index according to the order of their retention time in the chromatogram. After compound selection, a quantifier and a qualifier ion were designated. The quantifier ion peaks underwent Gaussian smoothing and the signal of the corresponding compound was measured by calculating the area beneath the smoothed curve. Ultimately, the data were adjusted for the total signal of the peak areas, resulting in relative abundances, which facilitated a more accurate comparison with the SIFT-MS and PTR-TOF-MS data. The total signal peak area was included in the dataset as an additional variable.

2.3.2. SIFT-MS

The SIFT-MS measurements were performed using a Voice200ultra (Syft Technologies, Christchurch, New Zealand). The carrier gas was helium and had a flow rate of 419.71 mL/min (5.32 torr L/s) with a flow tube pressure of 80.59 Pa (0.60 torr). The headspace was extracted from the sampling bag via a heated transfer line at 125 °C and the rate at which the headspace entered the flow tube was 23.68 mL/min (0.30 torr L/s). Sample product ions, generated by the three reagent ions H_3O^+, NO^+, and O_2^+, were scanned

over a range of 15 to 250 m/z. A sample measurement consisted of one preparation cycle and two sample cycles, with a maximum scanning time of 100 ms and a count limit of 10,000 counts per m/z. The total measurement time of one sample was approximately 3.5 min. At the beginning of each measurement day, a systematic validation routine was performed that involved measuring the composition of a calibrant gas consisting of seven compounds, including 1,2,3,4,5,6-hexafluorobenzene; 1,2,3,4,5-pentafluoro-6-(trifluoromethyl)benzene; 1,2,3,4-tetrafluoro benzene; 2-methylpropane; benzene; ethene; and toluene.

The raw signal intensities of the sample product ions were expressed in count rates (Hz) and were preprocessed following the approach of Benchennouf et al. (2023) to remove any instrument variation. This resulted in adjusted concentrations of the product ions. Next, the two sample cycles were averaged and similarly to the HSSE-GC-MS data, the individual variables were divided by the total product ion signal to allow for a better system comparison using the relative abundances. The total product ion signal was included in the dataset as an extra variable. During a later stage, the "identifier" tool in combination with the library of the LabSyft v1.6.2 software (Syft Technologies) was employed to tentatively identify compounds by linking the observed product ions to potential compounds of interest based on the full scan fingerprint. Furthermore, concentration estimations of VOCs selected by the HSSE-GC-MS were made using the library. In cases where the compound was not present in the library, the protonated ion generated by H_3O^+ was utilized with an average reaction rate coefficient (k-value) of 3.3×10^{-9} cm^3 s^{-1}. This k-value quantifies the rate at which the protonation between the reagent ion and the VOC occurs.

2.3.3. PTR-TOF-MS

The PTR measurements were executed using a PTR-TOF-MS 8000 (Ionicon Analytik, Innsbruck, Austria). The headspace was sampled from the bag at a flow rate of 25 mL/min via an insulated transfer line to the inlet of the drift tube of the device. The tube was operated at 600 drift voltage, 240 Pa, and 60.2 °C, resulting in a field density ratio (E/N) of 1.25×10^{-15} V cm^2 (125 Td). After being driven through the drift tube, sample product ions generated by the H_3O^+ reagent ions underwent mass separation in the time-of-flight module under a high vacuum of 8.8×10^{-5} Pa. Ion masses were scanned over a range from 1 to 318 m/z

with a sampling interval of 32 µs. Spectra were averaged at intervals of 5 s while each sample was measured for approximately 180 s. A comprehensive description of the spectrum mass range calibration and transmission curve construction can be found in a previous publication by Portillo-Estrada et al. (2021).

Next, a stable signal was selected for the individual egg spectra over a timeframe of 50 to 120 s and was subsequently averaged to create a single spectrum per egg. The spectra were cropped to a range from 15 to 318 m/z and the signal was integrated into nominal masses using the PTR-MS Viewer v3.4.4 software (Ionicon Analytik). Similar to the preprocessing approach described for the SIFT-MS, the raw signal intensities were converted into adjusted product ion concentrations to remove any instrument variation by assuming the nominal masses as compounds for which concentrations were estimated. This approach is also described by Granitto et al. (2007). Furthermore, the individual variables were divided by the total product ion signal to allow for better system comparison using relative abundances, and the total product ion signal was included in the dataset as an extra variable. Later, VOCs were identified in the spectra by fitting the peak of interest to a Gumbel curve using the "multipeak" tool (PTR-MS Viewer v3.4.4, Ionicon Analytik). The signal was then integrated to estimate the concentration using an average k-value of 2×10^{-9} $cm^3\ s^{-1}$ or specific linearly interpolated k-values were used in case compounds were reported in the work of Cappellin et al. (2012). For more information, refer to Portillo-Estrada et al. (2018).

2.4.Data analysis

The datasets were grouped per analytical technique for both days 2 and 8 separately. The HSSE-GC-MS dataset was double the size since the Twister® extractions were performed in duplicate during both the PTR- and the SIFT- measurements on the same day. Next, the datasets were randomized and divided into 6 equally divided splits for cross-validation. Each data split contained at least an observation for one of the three breeds and multiple measurements of the same egg were grouped within the same data split. Before starting the multivariate analysis, the variables were scaled to a zero mean and unit variance. All datasets from the three systems were analyzed by applying a partial least squares-discriminant analysis (PLS-DA) using the non-linear iterative partial least squares (NIPALS) algorithm. The relative abundances of the

VOCs or the product ions were set as predictor variables and the egg breed as a categorical response variable. The multivariate statistics were performed in Matlab v2018b (Mathworks, Natick, MA) using the PLS toolbox v8.7 2019 (Eigenvector Research, Wenatchee, WA) and by using The Unscrambler v10.3 (CAMO Software, Norway). The number of latent variables was determined by examining the scree plot to identify the components that accounted for the greatest variance, as well as by examining the root mean square error plot of the cross-validation set (RMSECV) to identify the point where the improvement in the model became negligible. The outlier analysis was conducted by examining the Q residuals and the Hotelling T^2, and by manually checking the data for aberrant spectra.

The PLS-DA models were further optimized by applying three different variable selection methods. First, variable importance in projection (VIP) was used, whereby each variable was considered significant if its score was 1 or higher for each of the three breeds. Second, forward interval partial least squares (FiPLS) was applied, whereby the number of variables was automatically chosen for a minimal RMSECV. Finally, the jackknifing approach was used to calculate weighted beta coefficients for variables to select those that contributed significantly to explaining the variation in the data (with $P < 0.05$). The first two approaches were performed in the PLS toolbox whereas the last approach was performed using The Unscrambler. The models having the highest balanced accuracy for egg breed on the cross-validation were selected. This balanced accuracy represented the average sensitivity across all classes and allowed for model comparison in the context of multiclass classification with imbalanced datasets. The sensitivity was calculated by dividing the number of true positives by the sum of the true positives and the false negatives.

3. Results & discussion

3.1. Comparative analysis of VOC data layout

From the 45 measured samples, only 30 were eventually considered for data analysis due to 3 unfertilized samples and 9 samples with dead embryos. It is possible that the transportation and sampling procedures caused damage to the embryos around day 2, as indicated by mortality between days 2 and 5 according to

breakout analysis. Nevertheless, the surviving embryos exhibited healthy development and were included in the analysis. Furthermore, the last 3 samples were identified as outliers due to measurement or processing errors and were excluded from the dataset. This resulted in a final dataset of 11 Dekalb, 11 Ross, and 8 Shaver eggs.

3.1.1. HSSE-GC-MS VOC identification

A total of 111 VOCs were identified from the GC-MS analysis, which could be further categorized into 14 different chemical classes (Fig. 2A). These identified VOCs are reported in detail in the overview table in Appendix A. Esters and alcohols were the most abundant VOCs and counted a total of 45 out of 111 compounds. This observation was similar to the observations of Borras et al. (2023) where the authors also used Twisters® and in which half of the identified VOCs were esters (11 out of 34) and alcohols (7 out of 34). This was in contrast to Xiang et al. (2019), where the authors used SPME fibers as sorbent materials. In their work, aldehydes were the most abundant class and consisted of 6 out of 18 VOCs. Furthermore, they identified only 2 alcohols and no esters. The dissimilarities observed may be attributed to variations in adsorption affinities between Twisters® and SPME fibers. Furthermore, the greater sensitivity of Twisters®, as reported by Tienpont et al. (2000), could have played a role in the higher number of VOCs detected using Twisters®. Additionally, the longer extraction time of 2 h employed in our study relative to the 3 min applied by Borras et al. (2023) potentially contributed to the identification of a larger number of VOCs.

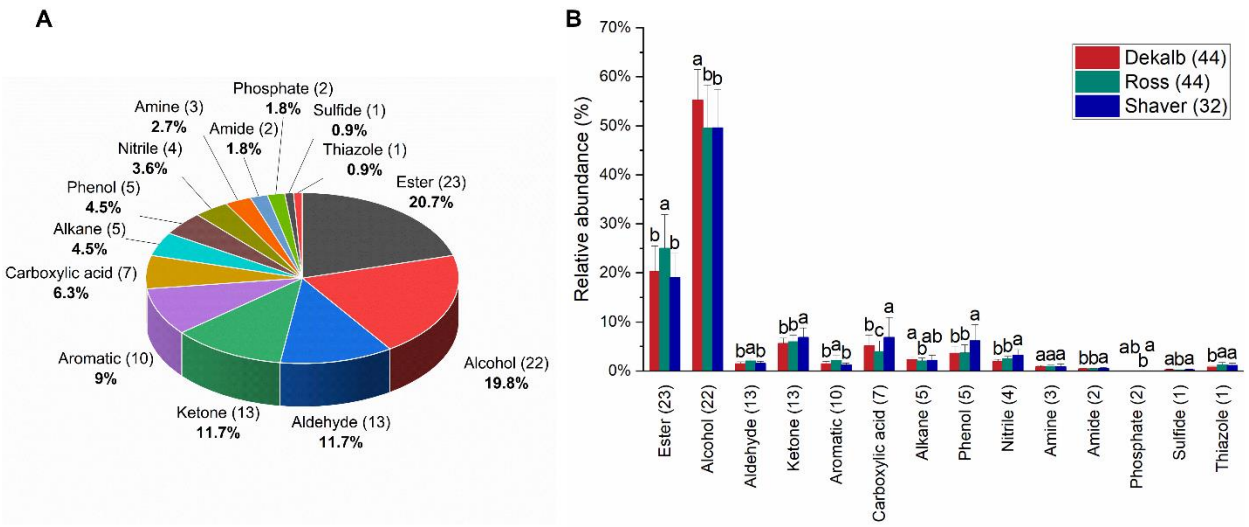

Fig. 2. Distribution of the VOC data from the HSSE-GC-MS into chemical classes. (A) Pie chart of the distribution of the number of compounds per chemical class, expressed in absolute number (between parentheses) and relative percentage to the total of 111 VOCs. (B) The relative abundance per chemical class per breed. The absolute number of VOCs per chemical class is presented in between parentheses and the average relative abundance of the signal per chemical class to the total VOC signal is presented on the vertical axis. The total number of observations per breed is noted in between parentheses. Pairwise t-tests were performed to compare the means and statistically significant differences within a class are indicated with a different letter ($P < 0.05$). The standard deviation is indicated with an error bar

Next, the relative abundance of the chemical classes per breed was studied and is depicted in Fig. 2B. It was observed that the alcohols covered approximately half of the total egg's VOC signal. This higher prevalence of alcohols was predominantly attributed to the signal of 1[2-(1-Butoxypropoxy)propoxy]propan-1-ol and 2-(2-Hydroxyethoxy)ethanol (Appendix Fig. B1). Both alcohols were assumed to have a synthetic origin since they were not reported yet as originating from living organisms and they are known to be used as solvents in gel formation (Dey et al., 2014; Shrivastava & Das, 2019). It is hypothesized that synthetic VOCs may originate from substances taken up by the mother hen, which are subsequently deposited in the egg. This concept of chemical contamination through feed or the environment has been demonstrated in multiple studies (Brambilla et al., 2009; Hoogenboom et al., 2016; Jondreville et al., 2017). On the other hand, the eggs themselves can potentially absorb odors from the environment and release them afterward (Webster et al., 2015; Xiang et al., 2018). Furthermore, the esters were significantly higher in abundance in Ross eggs. Esters can originate from plants and their presence

335 can be linked to the use of feed additives (Protasiuk & Olejnik, 2020). Finally, since the esters and alcohols
336 were respectively higher in relative abundance in Ross and Dekalb, Shaver had a higher relative abundance
337 in other classes such as ketones, carboxylic acids, phenols, nitriles, and amides.

338 ### 3.1.2. PTR-TOF-MS and SIFT-MS spectra characterization

339 An average egg signal of the PTR-TOF-MS and SIFT-MS data is presented in Fig. 3. The PTR data was
340 collected over a mass range from 15 to 318 m/z using the H_3O^+ reagent ion (Fig. 3A), whereas the SIFT
341 data was collected over a smaller 15 to 250 m/z range using the H_3O^+, NO^+, and O_2^+ reagent ions (Fig. 3B,
342 C and D, respectively). On one hand, the capability of the SIFT to use different reagent ions supported
343 compound identification by differentiating between isomeric classes. For instance, it can distinguish
344 between aldehydes and ketones, or acids and esters, even when they have the same molecular formula but
345 a distinct arrangement of atoms (Biasioli et al., 2011). On the other hand, the PTR was expected to have a
346 higher sensitivity since the time-of-flight module allowed for a high time resolution, resulting in almost
347 instantaneous detection of all compounds through full-spectrum acquisition. Furthermore, the high mass
348 accuracy allowed for distinguishing compounds with the same unit mass (i.e., isobaric compounds).

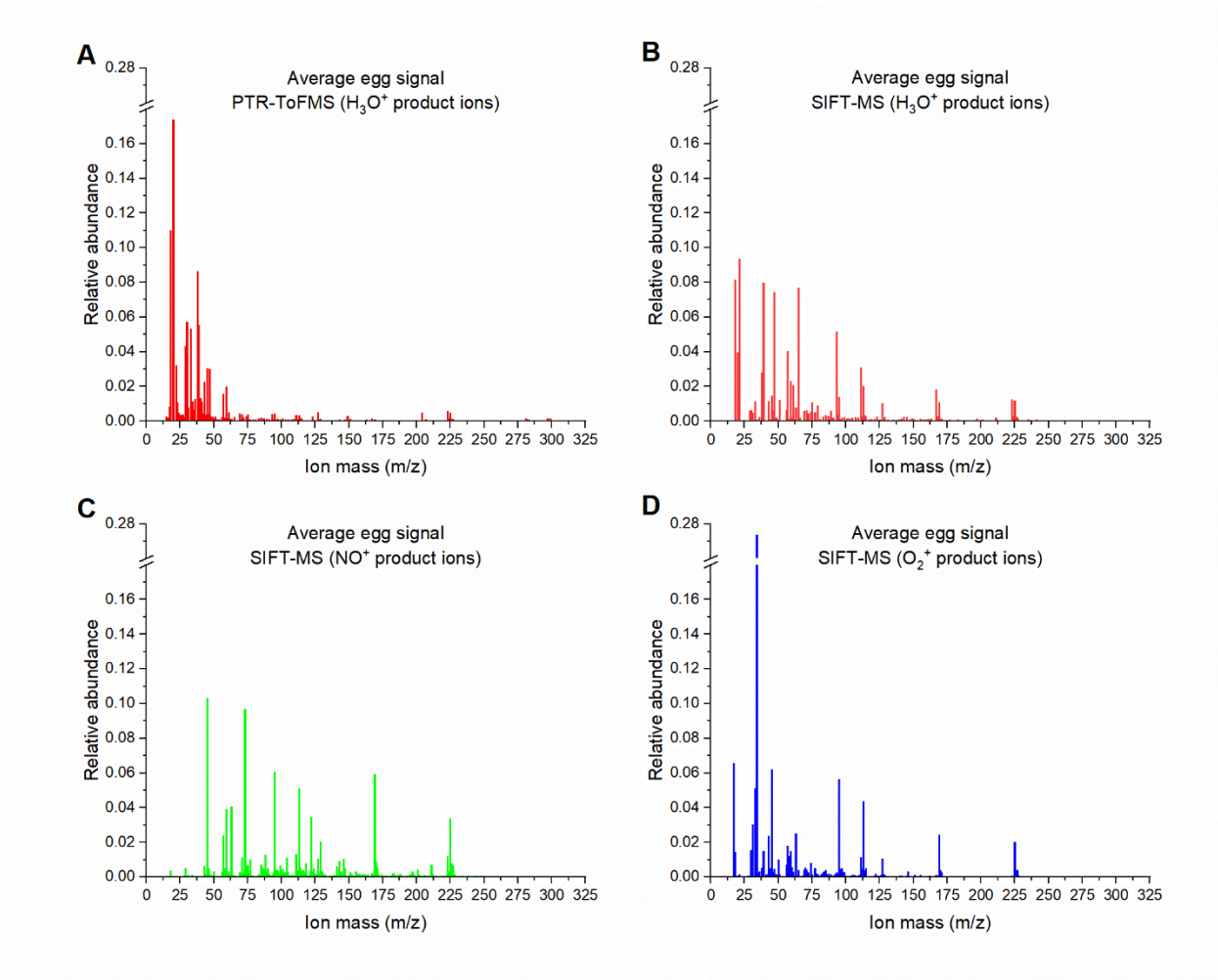

Fig. 3. Relative abundance of the ion masses of average egg signals on (A) the PTR-TOF-MS using the H_3O^+ reagent ion, (B) the SIFT-MS using the H_3O^+ reagent ion, (C) the SIFT-MS using the NO^+ reagent ion, and (D) the SIFT-MS using the O_2^+ reagent ion

When comparing the product ions of the H_3O^+ spectra, it was observed that the ion masses of the PTR data (Fig. 3A) were more abundant in the lower mass region than the ion masses of the SIFT data (Fig. 3B, C, and D). Possibly, this could be explained by sensitivity differences between the two devices towards lower and higher masses. Moreover, it is noteworthy that the PTR's transfer line was only insulated and not heated, which could have resulted in adsorption effects of heavier VOCs on the surface. Finally, high relative abundances were observed around product ion masses 223, 225 (H_3O^+), 225 (NO^+), and 225 (O_2^+). These masses corresponded with 2,2,4,4,6,6-hexamethyl-1,3,5,2,4,6-trioxatrisilinane which originated from the PDMS-Twisters® that were enclosed in the sampling bags together with the eggs.

For a better comparison between the two devices, the Pearson correlation coefficient was calculated on the adjusted product ion concentrations of the H_3O^+ ion masses within the 15 to 250 m/z range. These correlations are depicted in Fig. 4A and compounds that correlated higher than 0.5 are indicated with their ion mass. A total of 15 ion masses had a correlation coefficient exceeding 0.5, with the lower masses yielding the highest values. Furthermore, the mass spectra of the PTR-TOF-MS data were used to identify the corresponding compounds from these 15 ion masses. An overview of these compounds is given in Table B1 of Appendix B. As demonstrated for ion mass 47 in Fig. 4B, the signal can correspond with the presence of multiple compounds (this was also the case for ion masses 49, 57, 85, and 123; see Table B1 in Appendix B). In this case, both formic acid and ethanol share the same protonated ion mass. When individually quantifying the compound signals from the PTR-TOF-MS spectra, it was revealed that the ethanol abundance was dominating the signal of mass 47 and thereby causing a good correlation between the two devices (Fig. B2 in Appendix B). In Fig B2, it was also observed that the ethanol abundance was much higher on day 2 relative to day 8. This discrepancy can be plausibly attributed to the ethanol cleaning of the eggshell prior to the experiment. Nevertheless, the product ion masses corresponding with ethanol were retained in the dataset since they could overlap with other relevant compounds and it could be checked in a second phase whether the selection of a product ion mass was attributed to the presence of ethanol or not.

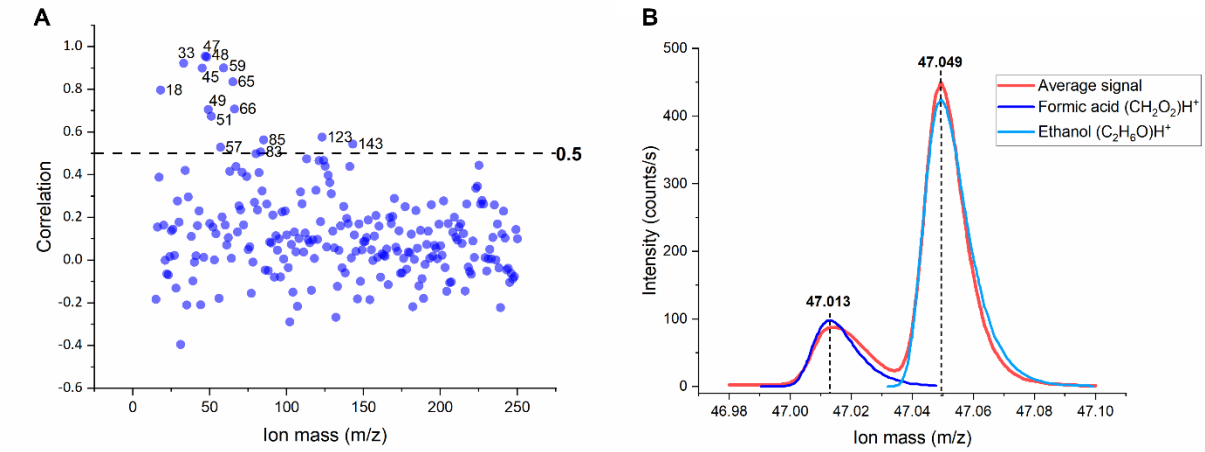

Fig. 4. (A) Correlation between the H_3O^+ product ion masses from the PTR-TOF-MS and the SIFT-MS. The correlation was calculated on the adjusted product ion concentrations. A threshold of 0.5 was set and ion masses showing correlations above this threshold are labeled. (B) Average signal of the ion mass 47 that had the highest correlation between PTR-TOF-MS and SIFT-MS data. This demonstrates the possibility of the PTR-TOF-MS to discriminate compounds based on their exact mass

As mentioned previously, the ability to differentiate exact compound masses enables the researcher to make a reliable estimation for the identification of the measured VOCs. Furthermore, compound identification can be facilitated and verified through the use of an online library of the most common VOCs generated through proton-transfer reactions by H_3O^+ ions (Pagonis et al., 2019). Similarly, the identifier tool within the LabSyft® software (Syft Technologies) permits SIFT-MS users to estimate the identity of a compound by analyzing the ratios of product ions generated by the different reagent ions. However, it was observed that formic acid and ethanol share the same product ion masses for both the three reagent ions and could thereby not be discriminated from one another using the SIFT-MS. It is also important to mention that the accuracy of the identification is constrained by the library content, which relies on the contributions made by the users who compiled the library.

3.2.Breed recognition based on VOCs

3.2.1. PLS-DA models for breed recognition

PLS-DA models were built to assess the performance of the different VOC analysis systems in distinguishing the three breeds. Initially, the analysis was performed on the full dataset of the device, and then variable selection methods were employed to eliminate less important compounds and enhance model performance. An overview of these classification models and their prediction- and balanced accuracies are presented in Table 1.

Table 1

PLS-DA models for breed recognition using different VOC analysis systems

VOC analysis system	Variable selection method	Number of factors	Number of variables	Prediction accuracy on cross-validation			Balanced accuracy †
				Dekalb	Ross	Shaver	
HSSE-GC-MS	full data	6	112	94.9%	89.4%	94.6%	91.9%
HSSE-GC-MS	FiPLS	7	11	96.4%	94.8%	97.7%	95.5% *
HSSE-GC-MS	VIP	6	12	95.1%	91.7%	92.9%	90.8%
HSSE-GC-MS	jackknifing	4	12	96.9%	91.5%	93.9%	95.2%
PTR-TOF-MS	full data	10	300	85.6%	95.5%	96.6%	90.9%
PTR-TOF-MS	FiPLS	3	5	96.1%	91.9%	96.6%	95.5% *
PTR-TOF-MS	VIP	6	35	95.1%	90.2%	97.7%	95.5%
PTR-TOF-MS	jackknifing	6	6	93.4%	88.3%	95.7%	91.9%
SIFT-MS	full data	2	695	52.4%	73.6%	71.3%	53.6%
SIFT-MS	FiPLS	4	11	94.7%	94.1%	90.3%	92.8% *
SIFT-MS	VIP	3	57	70.0%	90.2%	84.7%	80.7%
SIFT-MS	jackknifing	1	15	86.6%	65.0%	73.9%	79.6%

Note: † The balanced accuracy is calculated by taking the average of the sensitivities (number of true positives divided by the sum of the true positives and the false negatives). * An asterisk is used to indicate the best model per VOC analysis system based on the balanced accuracy.
Abbreviations: PLS-DA, partial least squares-discriminant analysis; FiPLS, forward interval partial least squares; VIP, variable importance projection; HSSE-GC-MS, headspace sorptive extraction gas chromatography-mass spectrometry; PTR-TOF-MS, proton transfer reaction time-of-flight mass spectrometry; SIFT-MS, selected ion flow tube mass spectrometry

Overall, the FiPLS variable selection approach generated models with the highest balanced accuracies. Possibly, the FiPLS managed better to obtain the best combination of relevant variables in the model due to its stepwise forward selection of only variables that reduce the RMSECV (Nørgaard et al., 2000). In case a variable is already included in the model, other variables that are correlated will not be taken up anymore since they will not bring added value to the model. This is in contrast to the VIP and jackknifing whereby variables are independently assessed (Chong & Jun, 2005; Martens & Martens, 2000). As a result, this independent variable assessment regardless of correlations may lead to the inclusion of variables that do not provide additional improvement of the model's performance.

The highest discrimination among the three breeds was achieved using the HSSE-GC-MS and the PTR-TOF-MS data, resulting in a balanced accuracy of 95.5%. The balanced accuracy of the best SIFT-MS model was 92.8%. Both the HSSE-GC-MS and the SIFT-MS FiPLS models were built with 11 variables,

421 whereas the PTR-TOF-MS FiPLS model was built with only 5 variables. These results indicate that all
422 three systems were able to successfully differentiate the three breeds.

423 Confusion matrices from the best performing PLS-DA models are presented in Fig. 5 to study which breeds
424 were wrongly interchanged with another breed. Overall, the predicted classes were well corresponding with
425 the actual classes for all breeds on all devices. It was observed that for all three devices, a certain number
426 of Ross breeds were wrongly categorized as a Shaver breed. Furthermore, the highest number of
427 misclassifications was observed for Ross being interchanged with Dekalb for the PTR-TOF-MS data. On
428 the other hand, all Dekalb and Shaver observations were well classified (Fig. 5B).

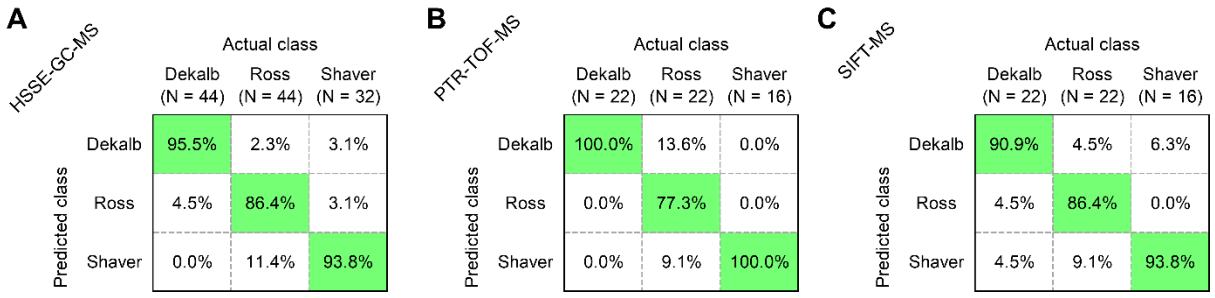

429

430 **Fig. 5.** Confusion matrices of the PLS-DA models to separate three different breeds of eggs based on their
431 VOC profile. The best models were selected per VOC analysis system and were obtained through an FiPLS
432 variable selection. The columns of the actual classes are presented as percentages of the total number of
433 observations per breed. This allows for a fair comparison between the three devices, despite their varying
434 number of observations. The three VOC analysis systems were respectively (A) HSSE-GC-MS, (B) PTR-
435 TOF-MS, and (C) SIFT-MS

436

3.2.2. Selected variables for breed distinction

For each VOC analysis system, biplots were generated to visualize the distinction of the breeds along the first two factors of their best PLS-DA models (Fig. 6). Moreover, the selected variables and their contributions to the separation are displayed through vectors that indicate both the magnitude and direction of their influence. Finally, the compounds related to the variables of the PTR-TOF-MS and SIFT-MS data were estimated using the exact masses from the time-of-flight spectra and the LabSyft® identifier tool, respectively. This is presented in Table 2 together with the relative abundance of the compounds per breed and their possible origin.

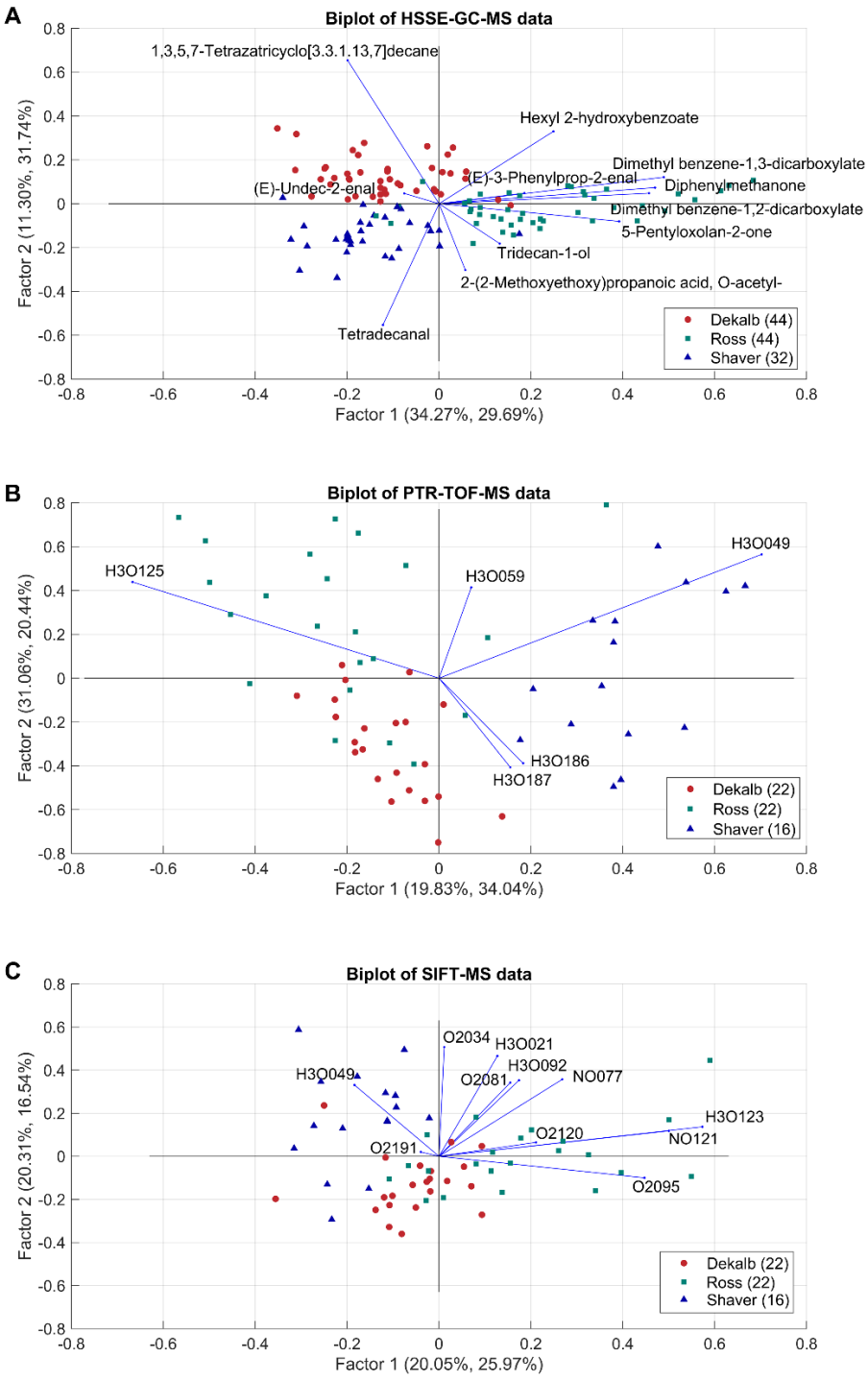

Fig. 6. Biplots of the PLS-DA models to separate three different breeds of eggs based on their VOC profile. The best models were selected per VOC analysis system and were obtained through an FiPLS variable selection for which the variables were labeled on the biplot. The percentage of X and Y variance per factor is presented in parentheses. The number of observations per breed is indicated in parentheses next to each respective breed. The product ions are noted together with the reagent ion they were generated with. For instance, H3O049 concerns ion mass 49 m/z from the H_3O^+ reagent ion The three VOC analysis systems were respectively (A) HSSE-GC-MS, (B) PTR-TOF-MS, and (C) SIFT-MS

Table 2

Selected variables from the PLS-DA models of the three devices and their average relative abundances and possible origin

Device	Variable and/or related compound	MF	MW	Chemical class	Relative abundance mean ± SE			Possible sources described in the literature	Reference
					Dekalb	Ross	Shaver		
HSSE-GC-MS	(E)-3-Phenylprop-2-enal	$C_9H_{12}O$	136	Alcohol	1.43 ± 0.10 x $10^{-3(b)}$	2.17 ± 0.11 x $10^{-3(a)}$	1.35 ± 0.13 x $10^{-3(b)}$	Can be used as a dietary supplement for laying hens to improve performance	(Wang et al., 2022)
	1,3,5,7-Tetrazatricyclo[3.3.1.1^{3,7}]decane	$C_6H_{12}N_4$	140	Alkane	4.35 ± 0.36 x $10^{-3(a)}$	1.21 ± 0.09 x $10^{-3(b)}$	1.41 ± 0.26 x $10^{-3(b)}$	Substance used in veterinary drugs, for instance for coccidiosis treatment	(Xu et al., 2017)
	5-Pentyloxolan-2-one	$C_9H_{16}O_2$	156	Ester	4.03 ± 0.19 x $10^{-3(b)}$	5.72 ± 0.28 x $10^{-3(a)}$	4.28 ± 0.24 x $10^{-3(b)}$	NA	
	(E)-Undec-2-enal	$C_{11}H_{20}O$	168	Aldehyde	2.66 ± 0.09 x $10^{-4(a)}$	2.18 ± 0.08 x $10^{-4(b)}$	2.60 ± 0.07 x $10^{-4(a)}$	Autoxidation product from oleic acid, an unsaturated fatty acid	(Belitz et al., 2009)
	Diphenylmethanone	$C_{13}H_{10}O$	182	Ketone	4.75 ± 0.23 x $10^{-3(b)}$	7.29 ± 0.38 x $10^{-3(a)}$	4.36 ± 0.23 x $10^{-3(b)}$	NA	
	2-(2-Methoxyethoxy)propanoic acid, O-acetyl-	$C_8H_{14}O_5$	190	Carboxylic acid	4.97 ± 0.41 x $10^{-2(b)}$	6.47 ± 0.61 x $10^{-2(a)}$	4.52 ± 0.43 x $10^{-2(b)}$	NA	
	Dimethyl benzene-1,2-dicarboxylate	$C_{10}H_{10}O_4$	194	Ester	2.49 ± 0.13 x $10^{-3(b)}$	3.81 ± 0.21 x $10^{-3(a)}$	2.26 ± 0.13 x $10^{-3(b)}$	Originally chemicals that are added to plastics to enhance flexibility. These lipophylic substances can be ingested by animals and accumulate in fat tissues or even eggs	(Kuzukiran et al., 2018)
	Dimethyl benzene-1,3-dicarboxylate	$C_{10}H_{10}O_4$	194	Ester	4.60 ± 0.19 x $10^{-2(b)}$	7.77 ± 0.40 x $10^{-2(a)}$	3.65 ± 0.21 x $10^{-2(c)}$		
	Tridecan-1-ol	$C_{13}H_{28}O$	200	Alcohol	1.73 ± 0.06 x $10^{-3(b)}$	1.82 ± 0.06 x $10^{-3(ab)}$	1.96 ± 0.05 x $10^{-3(a)}$	Earlier found in the preen oil of birds	(Amo et al., 2012; Whittaker & Hagelin, 2021)
	Tetradecanal	$C_{14}H_{28}O$	212	Aldehyde	4.24 ± 0.10 x $10^{-4(b)}$	4.46 ± 0.13 x $10^{-4(b)}$	5.52 ± 0.24 x $10^{-4(a)}$	Earlier found in the feathers and preen oil of birds	(Campagna et al., 2012)
	Hexyl 2-hydroxybenzoate	$C_{13}H_{18}O_3$	222	Ester	4.54 ± 0.29 x $10^{-3(a)}$	4.46 ± 0.33 x $10^{-3(a)}$	2.75 ± 0.16 x $10^{-3(b)}$	A salicylate that has been used as an anti-inflammatory drug from which residues can remain	(Protasiuk & Olejnik, 2020)
PTR-TOF-MS	Ethanol, second isotope [H3O049]	C_2H_6O	46	Alcohol	1.55 ± 0.04 x $10^{-3(c)}$	2.29 ± 0.14 x $10^{-3(b)}$	3.17 ± 0.19 x $10^{-3(a)}$	Can be a deterioration volatile from eggs. Although here, it is likely to be originating from the shell cleaning*	(Brown et al., 1986)
	Methanethiol [H3O049]	CH_4S	48	Thiol	1.55 ± 0.04 x $10^{-3(c)}$	2.29 ± 0.14 x $10^{-3(b)}$	3.17 ± 0.19 x $10^{-3(a)}$	Volatile found in the manure of laying hens	(Saksrithai & King, 2020)
	Propan-2-one [H3O059]	C_3H_6O	58	Ketone	1.95 ± 0.14 x $10^{-2(a)}$	1.95 ± 0.10 x $10^{-2(a)}$	2.06 ± 0.14 x $10^{-2(a)}$	Can be a deterioration volatile from eggs	(Brown et al., 1986)
	[H3O125]		NA		5.45 ± 0.13 x $10^{-4(b)}$	6.96 ± 0.30 x $10^{-4(a)}$	4.80 ± 0.09 x $10^{-4(c)}$	NA	
	[H3O186]		NA		6.90 ± 0.14 x $10^{-5(a)}$	6.60 ± 0.71 x $10^{-5(a)}$	6.97 ± 0.16 x $10^{-5(a)}$	NA	
	[H3O187]		NA		7.97 ± 0.21 x $10^{-5(a)}$	7.59 ± 0.24 x $10^{-5(a)}$	8.00 ± 0.21 x $10^{-5(a)}$	NA	

SIFT-MS	Hydronium, primary isotope [H3O021]	$H_3{}^{18}O^+$	21	NA	$9.17 \pm 0.44 \times 10^{-2(a)}$	$9.08 \pm 0.38 \times 10^{-2(a)}$	$9.94 \pm 0.60 \times 10^{-2(a)}$	NA	
	[O2034]		NA		$2.68 \pm 0.09 \times 10^{-1(b)}$	$2.64 \pm 0.06 \times 10^{-1(b)}$	$2.95 \pm 0.12 \times 10^{-1(a)}$	NA	
	Ethanol, second isotope [H3O049]	C_2H_6O	46	Alcohol	$8.88 \pm 0.62 \times 10^{-4(c)}$	$7.87 \pm 0.17 \times 10^{-4(b)}$	$2.07 \pm 0.27 \times 10^{-3(a)}$	Can be a deterioration volatile from eggs. Although here, it is likely to be originating from the shell cleaning*	(Brown et al., 1986)
	Methanethiol [H3O049]	CH_4S	48	Thiol	$8.88 \pm 0.62 \times 10^{-4(c)}$	$7.87 \pm 0.17 \times 10^{-4(b)}$	$2.07 \pm 0.27 \times 10^{-3(a)}$	Volatile found in the manure of laying hens	(Saksrithai & King, 2020)
	[NO077]		NA		$8.20 \pm 0.76 \times 10^{-3(b)}$	$1.10 \pm 0.09 \times 10^{-2(a)}$	$1.09 \pm 0.10 \times 10^{-2(a)}$	NA	
	[O2081]		NA		$6.13 \pm 0.43 \times 10^{-4(a)}$	$7.51 \pm 0.58 \times 10^{-4(a)}$	$7.70 \pm 0.70 \times 10^{-4(a)}$	NA	
	Butane-1-thiol, primary isotope [H3O092]	$C_4H_{10}S$	90	Thiol	$1.48 \pm 0.24 \times 10^{-4(a)}$	$2.28 \pm 0.36 \times 10^{-4(a)}$	$2.16 \pm 0.33 \times 10^{-4(a)}$	Volatile that can originate from gut bacteria	(Löser et al., 2020)
	Methylsulfonylmethane [O2095]	$C_2H_6O_2S$	94	Sulfonyl	$5.67 \pm 0.43 \times 10^{-2(a)}$	$6.60 \pm 0.40 \times 10^{-2(a)}$	$4.22 \pm 0.43 \times 10^{-2(b)}$	Compound with microbial origin that naturally occurs in food and is present in poultry facilities	(He & Slupsky, 2014; Trabue et al., 2010)
	2-Hydroxybenzaldehyde [H3O123]	$C_7H_6O_2$	122	Aldehyde	$2.08 \pm 0.15 \times 10^{-3(b)}$	$3.23 \pm 0.29 \times 10^{-3(a)}$	$1.84 \pm 0.19 \times 10^{-3(b)}$	Compound that has been used as a feed additive	(Vendramini et al., 2016)
	2-Hydroxybenzaldehyde [NO121]	$C_7H_6O_2$	122	Aldehyde	$3.00 \pm 0.21 \times 10^{-3(b)}$	$4.95 \pm 0.54 \times 10^{-3(a)}$	$2.36 \pm 0.32 \times 10^{-3(b)}$		
	1-Phenylethanol [H3O123]	$C_8H_{10}O$	122	Alcohol	$2.08 \pm 0.15 \times 10^{-3(b)}$	$3.23 \pm 0.29 \times 10^{-3(a)}$	$1.84 \pm 0.19 \times 10^{-3(b)}$	Reduction product of 1-phenylethanone after through dehydrogenases from microorganisms	(Dong et al., 2016)
	1-Phenylethanol [NO121]	$C_8H_{10}O$	122	Alcohol	$3.00 \pm 0.21 \times 10^{-3(b)}$	$4.95 \pm 0.54 \times 10^{-3(a)}$	$2.36 \pm 0.32 \times 10^{-3(b)}$		
	1-Phenylethanone [O2120]	C_8H_8O	120	Ketone	$2.95 \pm 0.37 \times 10^{-4(a)}$	$3.86 \pm 0.48 \times 10^{-4(a)}$	$2.90 \pm 0.30 \times 10^{-4(a)}$	Found in swallow and quail eggs and has been measured before in a poultry facility	(Costanzo et al., 2016; Trabue et al., 2010; Webster et al., 2015)
	[O2191]		NA		$3.29 \pm 0.64 \times 10^{-4(a)}$	$2.52 \pm 0.67 \times 10^{-4(a)}$	$3.53 \pm 0.74 \times 10^{-4(a)}$	NA	

Note: * the ethanol presence in this study was plausibly predominantly originating from the ethanol cleaning of the eggshell. However, the second isotope of ethanol was very low abundant in comparison to methanethiol which shared the same ion mass of 49 (Fig. B3 in Appendix B). Therefore, this ion mass was retained in the model. Statistical significant differences from pairwise t-tests are indicated with different letters ($P < 0.05$)
Abbreviations: HSSE-GC-MS, headspace sorptive extraction gas chromatography-mass spectrometry; PTR-TOF-MS, proton transfer reaction time-of-flight mass spectrometry; SIFT-MS, selected ion flow tube mass spectrometry; MF, molecular formula; MW, molecular weight; SE, standard error; NA, not available

A good separation of the three breeds is observed on the biplot of the HSSE-GC-MS data (Fig. 6A). After conducting an extensive literature review of the potential origin of the selected VOCs, it was observed that volatiles might originate from both synthetic and natural sources. For instance, the compound 1,3,5,7-tetrazatricyclo[3.3.1.1^{3,7}]decane was significantly more abundant in Dekalb (Table 2). It is a substance that can be used as a veterinary drug for coccidiosis treatment (Xu et al., 2017). Presumably, drug or feed additive administration to laying hens might result in the presence of these compounds or their metabolized products in the eggs. Consequently, variations in management might affect the eggs' VOC profile. Similarly, (E)-3-phenylprop-2-enal; dimethyl benzene-1,2-dicarboxylate; and dimethyl benzene-1,3-dicarboxylate were considerably more abundant in Ross and were likely originating from synthetic sources as well (Table 2). Finally, hexyl 2-hydroxybenzoate was more abundant in Dekalb and Ross versus Shaver. This salicylate has been reported to be used as an anti-inflammatory drug from which it is known that residues may remain in meat and eggs after drug administration or feed intake (Protasiuk & Olejnik, 2020).

Considering the compounds with a potential natural origin, it was observed that (E)-undec-2-enal was more abundant for Dekalb, although it was not significantly higher compared to Shaver (Table 2). This compound can be an autoxidation product from the unsaturated fatty acid oleic acid (Belitz et al., 2009). Oleic acid has been found in egg yolks as the most abundant fatty acid and it was demonstrated to vary significantly in relative abundance between different breeds that were fed the same diet (Bunea et al., 2017). Potentially, this indicates how the genotype can influence the egg's VOC profile. Furthermore, tetradecanal was more abundant in Shaver and is a natural compound that has been found earlier in birds (Campagna et al., 2012). Finally, tridecan-1-ol was more abundant in Shaver and Ross versus Dekalb. This compound is a natural compound that has been earlier found in the preen oil in birds (Amo et al., 2012; Whittaker & Hagelin, 2021).

For the PTR-TOF-MS data, a relatively small set of five variables was sufficient for breed discrimination (Fig. 6B). The identification of associated compounds was possible for two variables (Table 2). These were ethanol and methanethiol for 49 m/z (H3O049) and propan-2-one for 59 m/z (H3O059). As earlier

mentioned, ethanol was plausibly originating from the ethanol shell cleaning prior to the experiment. However, its second isotope under ion mass 49 was only attributing for a very limited amount relative to methanethiol (Fig. B3 in Appendix B). Methanethiol was a volatile found in the manure of laying hens (Saksrithai & King, 2020), whereas propan-2-one was identified in the past as a VOC indicating deterioration in eggs (Brown et al., 1986). Subsequently, these natural compounds may suggest a comparatively lower quality of the batch of Shaver eggs relative to the Dekalb and Ross eggs. Additionally, the observation that the Shaver eggs had the highest number of unfertile and dead eggs could serve as an indication of this lower quality. However, care has to be taken with this assumption due to the limited number of 15 eggs per batch.

As previously mentioned, the lowest model performance was obtained with the SIFT-MS data with a balanced accuracy of 92.8% (Table 1). Furthermore, a stronger correlation was found between the variables in Fig. 6C since they grouped closer together for the first two factors when compared to the vectors for the HSSE-GC-MS and PTR-TOF-MS data. Similarly to the PTR, ion mass 49 m/z from the H_3O^+ reagent ion was more prominent in Shaver (ion mass related to ethanol and methanethiol). It is not surprising that this variable has been selected as well for the SIFT-MS given its good correlation between the two devices that has earlier been demonstrated in Fig. 4A.

In line with the HSSE-GC-MS data (Fig. 6A), selected variables from the SIFT-MS PLS-DA model could be linked to either a synthetic or a natural origin. Ion masses 123 m/z (H_3O^+ product ion) and 121 m/z (NO^+ product ion) correlated well on the biplot in the direction of Ross (Fig. 6C) and could correspond with 2-hydroxybenzaldehyde which has been reported as a compound being used as a feed additive (Vendramini et al., 2016). For the same ion masses, correspondence was found for 1-phenylethanol and this was also confirmed using the PTR-TOF-MS spectra with protonated masses (Fig. B3 in Appendix B). This VOC potentially had a natural origin (Table 2). Other compounds potentially originating from natural sources were tentatively identified from ion mass 95 m/z (O_2^+ product ion) that could correspond with

methylsulfonylmethane, whereas 120 m/z (O_2^+ product ion) could correspond with 1-phenylethanone, and 92 m/z (H_3O^+ product ion) that corresponded with the first isotope of butane-1-thiol (Table 2).

Overall, it was noted that the variables selected for the HSSE-GC-MS model possessed higher molecular weights than the PTR-TOF-MS or the SIFT-MS variables. Consequently, there could be multiple explanations for this observation. First, the Twister® might adsorb better the heavier VOCs. Second, the heavier VOCs might have adsorbed onto the wall of the transfer line of the direct trace gas mass spectrometer devices. Lastly, it is plausible that the direct trace gas mass spectrometer devices were less sensitive to molecules with higher molecular weights.

3.3. Comparison of the VOC analysis systems

3.3.1. Correlation between HSSE-GC-MS, PTR-TOF-MS, and SIFT-MS

In this section, a comparison is made between the HSSE-GC-MS and the direct trace gas mass spectrometers to assess their complementarity. In order to compare the devices, the focus was set on correlating the absolute peak areas of the selected variables from the HSSE-GC-MS (Fig. 6A) with their estimated concentrations from the PTR-TOF-MS and SIFT-MS data, respectively.

An overview of these correlations is presented in Fig. 7. The correlations were relatively low with an average correlation of 0.15 for the PTR-TOF-MS and 0.02 for the SIFT-MS. Most likely, this limited correlation was because of the complexity of the egg's headspace. The HSSE-GC-MS performs an extensive compound separation prior to reaching the mass spectrometer, whereas direct trace gas mass spectrometers face a significant risk of ion mass overlaps, which can impede accurate estimation of compound concentrations. This issue was observed in the PTR-TOF-MS data as well, despite the time-of-flight module successfully identifying peaks based on precise compound masses. However, these compounds still overlapped due to their proximity in terms of exact masses. This can be observed in Fig. B4 in Appendix B where an overview is presented of the peak selections. Concerning the SIFT-MS, alternative product ions from NO^+ or O_2^+ can be utilized. However, the availability of this information in

the Syft library® is crucial or it needs to be manually incorporated by measuring pure standards of the specific VOCs of interest. In this study, only 5-pentyloxolan-2-one and (E)-3-phenylprop-2-enal were already present in the library. The remaining compounds were added manually without measuring pure standards, considering the formation of their protonated ion based on an average reaction rate constant. The reaction rate constants and product ions can be found in Table B2 of Appendix B.

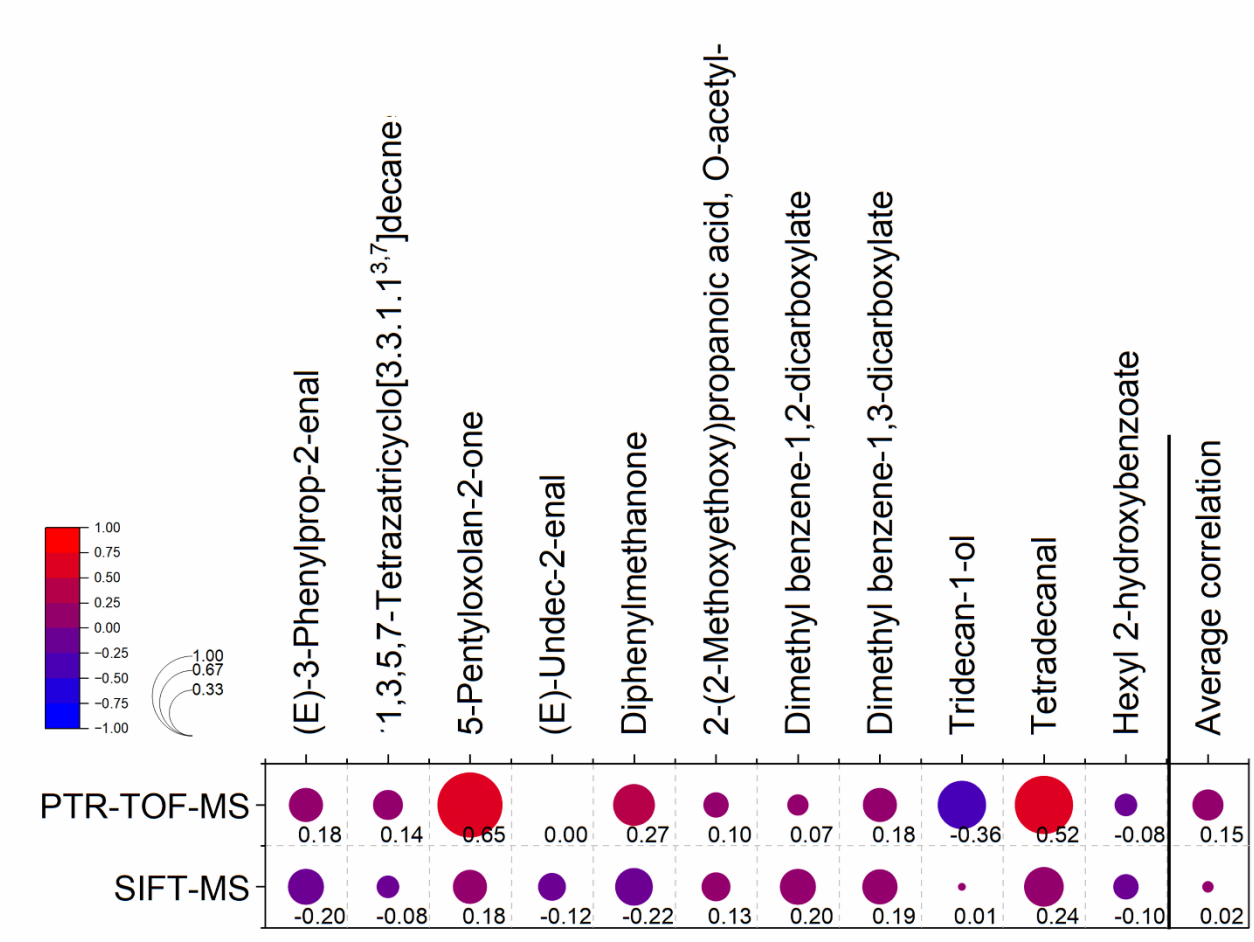

Fig. 7. Correlations between VOCs selected in the PLS-DA model for the HSSE-GC-MS using FiPLS variable selection and the concentration estimates of these VOCs via their corresponding ion masses in the PTR-TOF-MS and SIFT-MS data. The peak identifications from the PTR-TOF-MS data and the product ions from the SIFT-MS that were used to estimate the compound concentrations from the respective systems can be found in Fig. B4 and Table B2 of Appendix B, respectively.

In general, the PTR-TOF-MS exhibited the strongest correlations with the HSSE-GC-MS data. Specifically, the abundances of 5-pentyloxolan-2-one and tetradecanal showed relatively good correspondence. Although overlap was observed between compound signals (Fig B4 in Appendix B), the precise mass separation of VOCs on the PTR-TOF-MS enabled better isolation of individual compounds for quantification relative to the SIFT-MS. Achieving a strong correlation on the SIFT-MS proved to be more challenging due to the possibility of compounds overlapping under the same nominal mass, leading to more interference with each other. This suggests that the PTR-TOF-MS would be better suited for quantifying specific target compounds of interest that were identified using the HSSE-GC-MS. However, it has to be stated that the correlations were relatively low overall due to the complexity of the headspace. Towards future applications, the concentration estimates can be enhanced by constructing calibration curves for the compounds on the devices. Specifically, the SIFT-MS has the potential to improve when target scans are conducted, allowing for a longer integration time for the product ion masses of interest.

3.3.2. Summary of the comparison of the three VOC analysis systems

Based on the results of the current study, an overview table was created to compare the three VOC analysis systems for their user-friendliness and performance in creating breed distinction models (Table 3). Overall, the HSSE-GC-MS demonstrated the highest performance in identifying VOCs and generating accurate prediction models. However, it had a drawback in terms of its slow processing speed. On the other hand, the PTR-TOF-MS had the fastest processing speed and enabled effective identification through the separation of exact masses. The compound identification was the most difficult using the SIFT-MS because of the limited LabSyft library and the compound overlap on unit masses. Moreover, the model performance of the SIFT-MS was also the lowest. Finally, a significant finding was the complementarity in mass range selection of the VOCs by the systems. The HSSE-GC-MS distinction model primarily focused on heavier VOCs, while the direct trace gas analysis systems' models targeted lighter molecules. In summary, the overall consensus was that the combined use of HSSE-GC-MS and PTR-TOF-MS offered the most effective and complementary approach for comprehensively screening the full spectrum of egg VOCs.

Table 3

Comparison of the three VOC analysis systems for their user-friendliness and performance

Technique	User-friendliness			Breed distinction models	
	Total processing speed per sample	Identification	Sampling & Sensitivity (literature)	Performance model	Mass range selected compounds
HSSE-GC-MS	- 60 min (1 full scan)	+++ Column separation & Extensive NIST® library	Sorbent stir bar (Twister®) 0.1 – 1 ppb (Tienpont et al., 2000)	++ 95.5% balanced accuracy with 11 variables	136 to 222 g/mol
PTR-TOF-MS	+++ 3 min (36 full scans)*	++ Exact mass spectra & custom library through compound fitting	Direct headspace 0.01 – 0.1 ppb (Lehnert et al., 2019)	++ 95.5% balanced accuracy with 5 variables	± 46 to 186 g/mol
SIFT-MS	++ 3.5 min (3 full scans)	+ Compound overlap on unit masses & limited LabSyft library	Direct headspace 0.1 – 1 ppb (Lehnert et al., 2019)	+ 92.8% balanced accuracy with 11 variables	± 20 to 122 g/mol

Note: * The spectra of the PTR-TOF-MS were averaged in cycles of 5 s per cycle. The strength of the device for a certain feature was relatively expressed in the number of - and + symbols ranging from poor (-), to decent (+), to good (++), to excellent (+++).

Abbreviations: HSSE-GC-MS, headspace sorptive extraction gas chromatography-mass spectrometry; PTR-TOF-MS, proton transfer reaction time-of-flight mass spectrometry; SIFT-MS, selected ion flow tube mass spectrometry

4. Conclusion

In summary, our study assessed three VOC analysis systems for non-destructive separation of hatching eggs from three chicken breeds. HSSE-GC-MS identified 111 VOCs, with alcohols and esters being the most abundant. PTR-TOF-MS and SIFT-MS showed comparable spectra, but PTR-TOF-MS exhibited lower signal intensity for heavier ion masses. PLS-DA models demonstrated effective breed discrimination, with FiPLS variable selection performing the best across all systems. HSSE-GC-MS and PTR-TOF-MS achieved 95.5% balanced accuracy using a reduced set of 11 VOCs and 5 masses, respectively. SIFT-MS achieved 92.8% balanced accuracy. HSSE-GC-MS and the direct trace gas mass spectrometers exhibited complementary selectivity, with the former being more selective for higher molecular weights and the latter for lower molecular weight VOCs. The PTR-TOF-MS was suggested to be more suitable for quantifying compounds identified by the HSSE-GC-MS, unlike SIFT-MS. For future applications, calibration curves for target compounds are recommended to enhance concentration estimations. The literature review supported the idea of VOCs originating from both synthetic and natural sources. These findings highlight

the ability of these VOC analysis systems to perform egg quality control by non-destructively identifying variations in management practices or biological information encoded in eggs.

ACKNOWLEDGEMENTS

This work has received funding from the Flemish Environment Department, the Foundation for Food and Agricultural Research [EggTech-0000000028], and the Research Foundation – Flanders [SB project 1SC7219N and SB project 1S54823N]. Furthermore, gratitude is expressed to Elfie Dekempeneer for her support in performing the samplings.

DECLARATION OF INTEREST

All the authors declare that they have no conflict of interest.

DECLARATION OF GENERATIVE AI AND AI-ASSISTED TECHNOLOGIES IN THE WRITING PROCESS

During the preparation of this work, the authors used Chat-GPT in order to improve the manuscript's readability. After using this tool, the authors reviewed and edited the content as needed and take full responsibility for the content of the publication.

REFERENCES

Amo, L., Avilés, J. M., Parejo, D., Peña, A., Rodríguez, J., & Tomás, G. (2012). Sex recognition by odour and variation in the uropygial gland secretion in starlings. *Journal of Animal Ecology*, *81*(3), 605–613. https://doi.org/10.1111/j.1365-2656.2011.01940.x

Belitz, H.-D., Grosch, W., & Schieberle, P. (2009). Food Chemistry. In *Springer*. Springer Berlin Heidelberg. https://doi.org/10.1007/978-3-540-69934-7

Benchennouf, A., Corion, M., Dizon, A., Zhao, Y., Lammertyn, J., De Coninck, B., Nicolaï, B., Vercammen, J., & Hertog, M. (2023). Increasing the Robustness of SIFT-MS Volatilome Fingerprinting by Introducing Notional Analyte Concentrations. *Journal of the American Society for Mass Spectrometry*. https://doi.org/10.1021/jasms.3c00168

Biasioli, F., Yeretzian, C., Märk, T. D., Dewulf, J., & Van Langenhove, H. (2011). Direct-injection mass spectrometry adds the time dimension to (B)VOC analysis. *TrAC Trends in Analytical Chemistry*, *30*(7), 1003–1017. https://doi.org/10.1016/j.trac.2011.04.005

Borras, E., Wang, Y., Shah, P., Bellido, K., Hamera, K. L., Arlen, R. A., McCartney, M. M., Portillo, K., Zhou, H., Davis, C. E., & Turpen, T. H. (2023). Active sampling of volatile chemicals for non-invasive classification of chicken eggs by sex early in incubation. *PLOS ONE*, *18*(5), e0285726. https://doi.org/10.1371/journal.pone.0285726

Brambilla, G., Fochi, I., De Filippis, S. P., Iacovella, N., & Domenico, A. di. (2009). Pentachlorophenol, polychlorodibenzodioxin and polychlorodibenzofuran in eggs from hens exposed to contaminated wood shavings. *Food Additives & Contaminants: Part A*, *26*(2), 258–264. https://doi.org/10.1080/02652030802322572

Brown, M. L., Holbrook, D. M., Hoerning, E. F., Legendre, M. G., & ST. Angelo, A. J. (1986). Volatile Indicators of Deterioration in Liquid Egg Products. *Poultry Science*, *65*(10), 1925–1933.

https://doi.org/10.3382/ps.0651925

Bunea, A., Copaciu, F. M., Paşcalău, S., Dulf, F., Rugină, D., Chira, R., & Pintea, A. (2017). Chromatographic analysis of lypophilic compounds in eggs from organically fed hens. *Journal of Applied Poultry Research*, *26*(4), 498–508. https://doi.org/10.3382/japr/pfx022

Campagna, S., Mardon, J., Celerier, A., & Bonadonna, F. (2012). Potential semiochemical molecules from birds: A practical and comprehensive compilation of the last 20 years studies. *Chemical Senses*, *37*(1), 3–25. https://doi.org/10.1093/chemse/bjr067

Cappellin, L., Karl, T., Probst, M., Ismailova, O., Winkler, P. M., Soukoulis, C., Aprea, E., Märk, T. D., Gasperi, F., & Biasioli, F. (2012). On quantitative determination of volatile organic compound concentrations using proton transfer reaction time-of-flight mass spectrometry. *Environmental Science and Technology*, *46*(4), 2283–2290. https://doi.org/10.1021/es203985t

Cheng, S., Wang, Y., Wang, J., Wei, Z., & Lu, Q. (2010). Detection of Eggshell Crack using Electronic Nose. *Transactions of the ASABE*, *53*(3), 789–794. https://doi.org/10.13031/2013.30052

Chong, I.-G., & Jun, C.-H. (2005). Performance of some variable selection methods when multicollinearity is present. *Chemometrics and Intelligent Laboratory Systems*, *78*(1–2), 103–112. https://doi.org/10.1016/j.chemolab.2004.12.011

Costanzo, A., Panseri, S., Giorgi, A., Romano, A., Caprioli, M., & Saino, N. (2016). The odour of sex: Sex-related differences in volatile compound composition among barn swallow eggs carrying embryos of either sex. *PLoS ONE*, *11*(11), 1–17. https://doi.org/10.1371/journal.pone.0165055

Dey, A., Bera, B., Bera, R., & Chakrabarty, D. (2014). Influence of diethylene glycol as a porogen in a glyoxal crosslinked polyvinyl alcohol hydrogel. *RSC Adv.*, *4*(80), 42260–42270. https://doi.org/10.1039/C4RA04742G

Dong, F., Zhou, Y., Zeng, L., Peng, Q., Chen, Y., Zhang, L., Su, X., Watanabe, N., & Yang, Z. (2016).

Elucidation of Differential Accumulation of 1-Phenylethanol in Flowers and Leaves of Tea (Camellia sinensis) Plants. *Molecules*, *21*(9), 1106. https://doi.org/10.3390/molecules21091106

Granitto, P., Biasoli, F., Aprea, E., Mott, D., Furlanello, C., Mark, T., & Gasperi, F. (2007). Rapid and non-destructive identification of strawberry cultivars by direct PTR-MS headspace analysis and data mining techniques. *Sensors and Actuators B: Chemical*, *121*(2), 379–385. https://doi.org/10.1016/j.snb.2006.03.047

He, X., & Slupsky, C. M. (2014). Metabolic Fingerprint of Dimethyl Sulfone (DMSO 2) in Microbial–Mammalian Co-metabolism. *Journal of Proteome Research*, *13*(12), 5281–5292. https://doi.org/10.1021/pr500629t

Helmig, D., & Vierling, L. (1995). Water Adsorption Capacity of the Solid Adsorbents Tenax TA, Tenax GR, Carbotrap, Carbotrap C, Carbosieve SIII, and Carboxen 569 and Water Management Techniques for the Atmospheric Sampling of Volatile Organic Trace Gases. *Analytical Chemistry*, *67*(23), 4380–4386. https://doi.org/10.1021/ac00119a029

Hoogenboom, R. L. A. P., ten Dam, G., van Bruggen, M., Jeurissen, S. M. F., van Leeuwen, S. P. J., Theelen, R. M. C., & Zeilmaker, M. J. (2016). Polychlorinated dibenzo-p-dioxins and dibenzofurans (PCDD/Fs) and biphenyls (PCBs) in home-produced eggs. *Chemosphere*, *150*, 311–319. https://doi.org/10.1016/j.chemosphere.2016.02.034

Hua, Z., Yu, Y., Zhao, C., Zong, J., Shi, Y., & Men, H. (2021). A feature dimensionality reduction strategy coupled with an electronic nose to identify the quality of egg. *Journal of Food Process Engineering*, *44*(11). https://doi.org/10.1111/jfpe.13873

Jondreville, C., Cariou, R., Travel, A., Belhomme, L.-J., Dervilly-Pinel, G., Le Bizec, B., Huneau-Salaün, A., & Le Bouquin-Leneveu, S. (2017). Hens can ingest extruded polystyrene in rearing buildings and lay eggs contaminated with hexabromocyclododecane. *Chemosphere*, *186*, 62–67. https://doi.org/10.1016/j.chemosphere.2017.07.117

679 Kuzukiran, O., Yurdakok-Dikmen, B., Sevin, S., Sireli, U. T., Iplikcioglu-Cil, G., & Filazi, A. (2018).
680 Determination of selected endocrine disruptors in organic, free-range, and battery-produced hen eggs
681 and risk assessment. *Environmental Science and Pollution Research*, *25*(35), 35376–35386.
682 https://doi.org/10.1007/s11356-018-3400-5

683 Lee, S. W., La, T. M., Lee, H. J., Choi, I. S., Song, C. S., Park, S. Y., & Lee, J. B. (2019). Characterization
684 of microbial communities in the chicken oviduct and the origin of chicken embryo gut microbiota.
685 *Scientific Reports*, *9*(1), 1–11. https://doi.org/10.1038/s41598-019-43280-w

686 Lehnert, A.-S., Behrendt, T., Ruecker, A., Pohnert, G., & Trumbore, S. (2019). Performance of SIFT-MS
687 and PTR-MS in the measurement of volatile organic compounds at different humidities. *Atmospheric*
688 *Measurement Techniques Discussions*, *November*, 1–17. https://doi.org/10.5194/amt-2019-349

689 Liu, P., & Tu, K. (2012). Prediction of TVB-N content in eggs based on electronic nose. *Food Control*,
690 *23*(1), 177–183. https://doi.org/10.1016/j.foodcont.2011.07.006

691 Löser, B., Grabenschröer, A., Pugliese, G., Sukul, P., Trefz, P., Schubert, J. K., & Miekisch, W. (2020).
692 Changes of Exhaled Volatile Organic Compounds in Postoperative Patients Undergoing Analgesic
693 Treatment: A Prospective Observational Study. *Metabolites*, *10*(8), 321.
694 https://doi.org/10.3390/metabo10080321

695 Martens, H., & Martens, M. (2000). Modified Jack-knife estimation of parameter uncertainty in bilinear
696 modelling by partial least squares regression (PLSR). *Food Quality and Preference*, *11*(1–2), 5–16.
697 https://doi.org/10.1016/S0950-3293(99)00039-7

698 Nørgaard, L., Saudland, A., Wagner, J., Nielsen, J. P., Munck, L., & Engelsen, S. B. (2000). Interval Partial
699 Least-Squares Regression (i PLS): A Comparative Chemometric Study with an Example from Near-
700 Infrared Spectroscopy. *Applied Spectroscopy*, *54*(3), 413–419.
701 https://doi.org/10.1366/0003702001949500

Pagonis, D., Sekimoto, K., & de Gouw, J. (2019). A Library of Proton-Transfer Reactions of H 3 O + Ions Used for Trace Gas Detection. *Journal of the American Society for Mass Spectrometry*, *30*(7), 1330–1335. https://doi.org/10.1007/s13361-019-02209-3

Portillo-Estrada, M., Zenone, T., Arriga, N., & Ceulemans, R. (2018). Contribution of volatile organic compound fluxes to the ecosystem carbon budget of a poplar short-rotation plantation. *GCB Bioenergy*, *10*(6), 405–414. https://doi.org/10.1111/gcbb.12506

Portillo-Estrada, M., Van Moorleghem, C., Janssenswillen, S., Cooper, R. J., Birkemeyer, C., Roelants, K., & Van Damme, R. (2021). Proton-transfer-reaction time-of-flight mass spectrometry (PTR-TOF-MS) as a tool for studying animal volatile organic compound (VOC) emissions. *Methods in Ecology and Evolution*, *12*(4), 748–766. https://doi.org/10.1111/2041-210X.13554

Protasiuk, E., & Olejnik, M. (2020). Residues of salicylic acid and its metabolites in hen plasma, tissues and eggs as a result of animal treatment and consumption of naturally occurring salicylates. *Food Additives and Contaminants - Part A Chemistry, Analysis, Control, Exposure and Risk Assessment*, *37*(6), 946–954. https://doi.org/10.1080/19440049.2020.1744740

Rizzi, G. P. (2008). The Strecker Degradation of Amino Acids: Newer Avenues for Flavor Formation. *Food Reviews International*, *24*(4), 416–435. https://doi.org/10.1080/87559120802306058

Saksrithai, K., & King, A. J. (2020). Lactobacillus species in drinking water had no main effects on sulphur compounds from manure, egg quality, and selected serum parameters of second cycle hens. *British Poultry Science*, *61*(3), 328–335. https://doi.org/10.1080/00071668.2019.1709618

Shrivastava, S., & Das, A. (2019). Interaction between ethoxylated emulsifiers and propylene glycol based solvents: Gelation and rheology study. *Colloids and Surfaces A: Physicochemical and Engineering Aspects*, *582*(June), 123905. https://doi.org/10.1016/j.colsurfa.2019.123905

Smith, D., Španěl, P., Herbig, J., & Beauchamp, J. (2014). Mass spectrometry for real-time quantitative

725 breath analysis. *Journal of Breath Research*, *8*(2). https://doi.org/10.1088/1752-7155/8/2/027101

726 Tienpont, B., David, F., Bicchi, C., & Sandra, P. (2000). High capacity headspace sorptive extraction.
727 *Journal of Microcolumn Separations*, *12*(11), 577–584. https://doi.org/10.1002/1520-
728 667X(2000)12:11<577::AID-MCS30>3.0.CO;2-Q

729 Trabue, S., Scoggin, K., Li, H., Burns, R., Xin, H., & Hatfield, J. (2010). Speciation of volatile organic
730 compounds from poultry production. *Atmospheric Environment*, *44*(29), 3538–3546.
731 https://doi.org/10.1016/j.atmosenv.2010.06.009

732 Turner, C. (2016). Techniques and issues in breath and clinical sample headspace analysis for disease
733 diagnosis. *Bioanalysis*, *8*(7), 677–690. https://doi.org/10.4155/bio.16.22

734 Vendramini, T. H. A., Takiya, C. S., Silva, T. H., Zanferari, F., Rentas, M. F., Bertoni, J. C., Consentini,
735 C. E. C., Gardinal, R., Acedo, T. S., & Rennó, F. P. (2016). Effects of a blend of essential oils, chitosan
736 or monensin on nutrient intake and digestibility of lactating dairy cows. *Animal Feed Science and*
737 *Technology*, *214*, 12–21. https://doi.org/10.1016/j.anifeedsci.2016.01.015

738 Wang, Y., Wang, Y., Su, C., Wang, L., Lv, X., Cui, G., Ji, L., Huang, Y., Zhang, H., & Chen, W. (2022).
739 Dietary cinnamaldehyde with carvacrol or thymol improves the egg quality and intestinal health
740 independent of gut microbiota in post-peak laying hens. *Frontiers in Veterinary Science*, *9*.
741 https://doi.org/10.3389/fvets.2022.994089

742 Webster, B., Hayes, W., & Pike, T. W. (2015). Avian Egg Odour Encodes Information on Embryo Sex,
743 Fertility and Development. *PLOS ONE*, *10*(1), e0116345.
744 https://doi.org/10.1371/journal.pone.0116345

745 Whittaker, D. J., & Hagelin, J. C. (2021). Female-Based Patterns and Social Function in Avian Chemical
746 Communication. *Journal of Chemical Ecology*, *47*(1), 43–62. https://doi.org/10.1007/s10886-020-
747 01230-1

748 Xiang, X. le, Wang, Y. lan, Yu, Z. hui, Ma, M. hu, Zhu, Z. hui, & Jin, Y. guo. (2018). Non-destructive
749 characterization of egg odor and fertilization status by SPME/GC-MS coupled with electronic nose.
750 *Journal of the Science of Food and Agriculture*, *99*(7), 3264–3275. https://doi.org/10.1002/jsfa.9539

751 Xiang, X., Hu, G., Jin, Y., Jin, G., & Ma, M. (2022). Nondestructive characterization gender of chicken
752 eggs by odor using SPME/GC-MS coupled with chemometrics. *Poultry Science*, *101*(3), 101619.
753 https://doi.org/10.1016/j.psj.2021.101619

754 Xiang, X., Jin, G., Gouda, M., Jin, Y., & Ma, M. (2019). Characterization and classification of volatiles
755 from different breeds of eggs by SPME-GC–MS and chemometrics. *Food Research International*,
756 *116*(August 2018), 767–777. https://doi.org/10.1016/j.foodres.2018.09.010

757 Xiang, X., Wang, Y., Yu, Z., Ma, M., Zhu, Z., & Jin, Y. (2019). Non-destructive characterization of egg
758 odor and fertilization status by SPME/GC-MS coupled with electronic nose. *Journal of the Science of*
759 *Food and Agriculture*, *99*(7), 3264–3275. https://doi.org/10.1002/jsfa.9539

760 Xu, X., Duhoranimana, E., & Zhang, X. (2017). Selective extraction of methenamine from chicken eggs
761 using molecularly imprinted polymers and LC-MS/MS confirmation. *Food Control*, *73*, 265–272.
762 https://doi.org/10.1016/j.foodcont.2016.08.013

763 Yongwei, W., Wang, J., Zhou, B., & Lu, Q. (2009). Monitoring storage time and quality attribute of egg
764 based on electronic nose. *Analytica Chimica Acta*, *650*(2), 183–188.
765 https://doi.org/10.1016/j.aca.2009.07.049

766 Zhang, Q., Kang, S., Yin, C., Li, Z., & Shi, Y. (2022). An adaptive learning method for the fusion
767 information of electronic nose and hyperspectral system to identify the egg quality. *Sensors and*
768 *Actuators A: Physical*, *346*(June), 113824. https://doi.org/10.1016/j.sna.2022.113824